SUPPLEMENTARY MATERIAL

Estimating the absolute degree of aggregation:

The degree of aggregation has been defined as:

$$DA = \langle i(x,y)\rangle g(0,0) = c\,\frac{\langle N_M\rangle}{\langle N_E\rangle} \qquad \text{(S1)}$$

where the constant c depends on unknown optical and fluorescent probe parameters [1]. It can be determined experimentally by measuring the intensity and the correlation function of a sample with only monomers present since this would give $\langle N_m\rangle = \langle N_E\rangle$ and hence the product in Equation S1 is simply the constant, c.

In the past we have assumed that binding of non-specific antibodies with the same fluorescent probe should be a reasonable approximation of a monomeric distribution and this sample can then be used to estimate the constant c [2]. Since the intensity for this sample is low, it is important to account for the background intensity as well as the correlation function from a background sample – where we use a sample labeled with only the primary antibody as the control sample. In our cases, the $g(0,0)$ value for the primary antibody control sample was near zero and did not need to be accounted for. Using these samples, we find

$$c = \langle g_{sec}(0,0)\rangle * \left[\langle I_{avg.}(secondary)\rangle - \langle I_{avg.}(primary)\rangle\right] \qquad \text{(S2)}$$
$$= 0.05 * (7.76 - 5.63) = 0.11$$

for the 561 nm probe and our microscope configuration.

Using this approach for the samples used here, then allowed us to estimate the absolute degrees of aggregation shown in Table S1, which here is the average number of secondary antibodies bound per endosome,

Table S1: Average of Degrees of Aggregation for Cells Labelled for Marked Compartments in C2C12 and A549 Cells

	C2C12	**A549**
Marker	$\langle DA \rangle$	$\langle DA \rangle$
Rab5-561	1234	345
Rab7-633	930	654

In our measurements, the intensities from non-specific binding of LAMP-1 secondary antibodies were not significantly above the intensities from primary antibodies and hence the estimate of the constant c was not possible.

The data in Table S1 suggest that there are on the order of 1000 Rab5 and Rab7 per endosome in C2C12 cells and about half that many in A549 cells.

Estimating the effect of object convolution on the measured beam width:

The theory of ICS and its related experiments (ICCS, TRICCS) assumes that the fluorescence from the objects are point sources without any dimension so that the width of the calculated correlation functions are accurate measures of the width of the laser beam. In fact, in past work, this parameter has been used as an indication of the reliability of the ICS measurement [2]. In reality, the objects are not without dimension, so the calculated beam width from the experiments will reflect a convolution of the object with the laser beam. This is particularly evident in this work where the beam widths calculated from the ICS experiments are always greater than the theoretical ones. We can use this information to estimate the actual size of the objects in the sample.

First, we calculate the convolution of spherical objects of various radii, r, with the theoretical beam width as shown in Figure S1 (in one dimension only). Here r ranges from 0.75 to 2.25 times the theoretical beam width and is compared to the theoretical beam width.

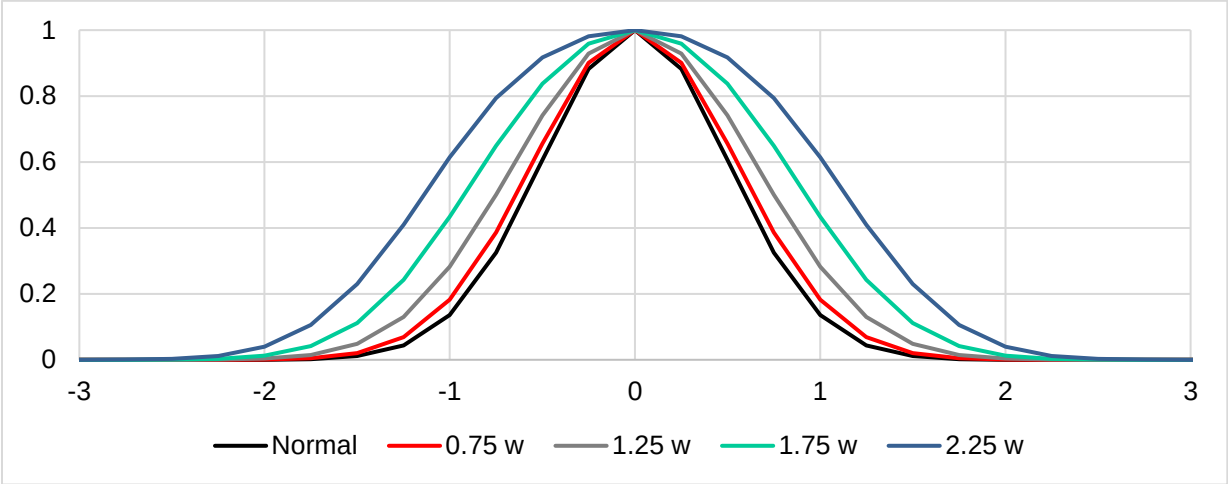

Figure S1 Effect of convolution on measured beam width

It is evident, that the effect of the convolution is small whenever the object radius is less than about 0.75 times the theoretical beam width. For larger radius objects, the convolutions still yield curves that are approximated well by a Gaussian function.

Second, we fit each of the convoluted functions to Gaussian functions to estimate a 'measured' beam width, and plotted that value as a function of the radius of the object as show in Figure S2:

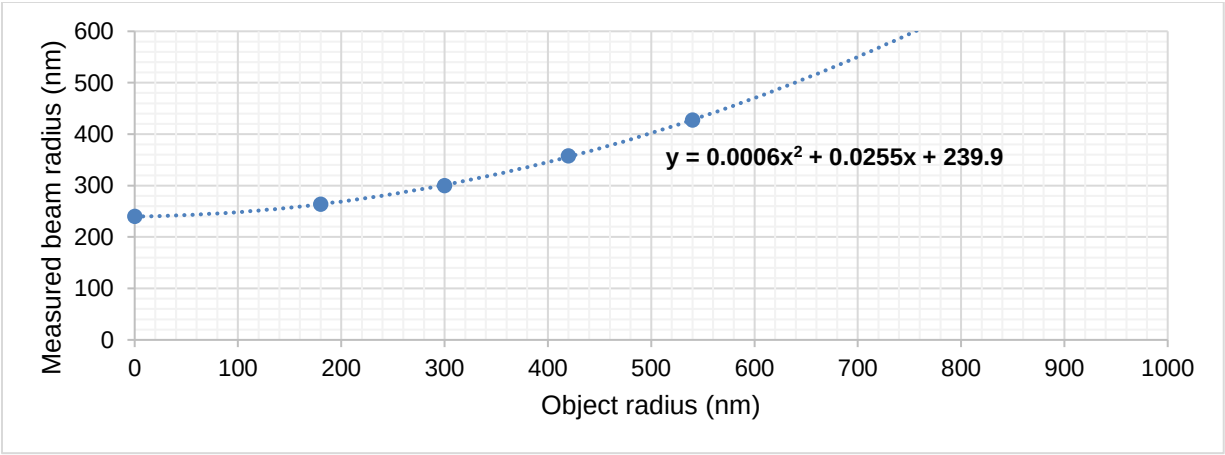

Figure S2: Experimental Fitted Laser Beam Width as a Function of Object Diameter

Third, using the curve in Figure S2, we use the actual measured beam widths to estimate the object sizes, here the endosome sizes, as reported in Table 2 of the main paper.

Control for Cross Reactivity of Antibodies in C2C12 Cells

To test for cross reactivity of antibodies, C2C12 cells were labelled using both primary and secondary antibodies against Rab7 (Figure S3 A_{top}, B_{top}, C_{top}) and LAMP-1 (Figure S3 A_{bottom}, D_{bottom}, E_{bottom}) or only primary antibodies (E_{top}, B_{bottom}) or secondary (D_{top}, C_{bottom}) antibodies as control. Similarly, they were labeled using both primary and secondary antibodies compared to four other samples prepared without the addition of one primary or secondary antibody, in various combinations. Figure S3 shows representative images from these experiments.

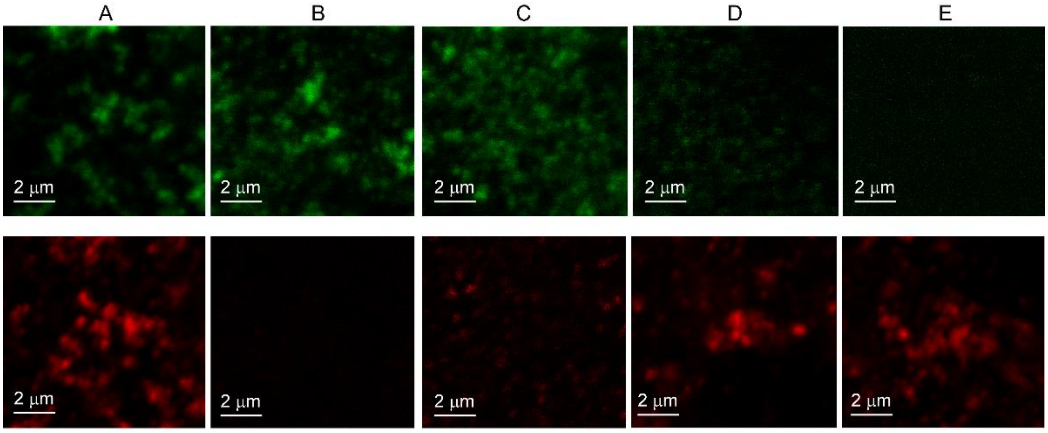

Figure S3: Images used to determine extent of cross reactivity of antibodies.

The control experiments with only primary antibodies have no fluorescence and those with only secondary antibodies have low fluorescence from non-specific binding. Table S2 shows the average intensities and correlation function amplitudes, with standard error, from ICS analysis of several images from different cells in these experiments.

Table S2: Average Intensities and Correlation Function Amplitudes in Cross Reactivity Experiments

Sample		A	B	C	D	E
Top	$\langle \boldsymbol{I_{avg.}} \rangle$	**173 ± 14**	**116 ± 11**	**108 ± 13**	21 ± 2	8.6 ± 0.1
	$\langle \mathbf{g(0,0)} \rangle$	0.62 ± 0.07	0.40 ± 0.09	0.36 ± 0.09	0.12 ± 0.02	0.01 ± 0.01
Bottom	$\langle \boldsymbol{I_{avg.}} \rangle$	**509 ± 92**	9.3 ± 0.2	15.4 ± 0.7	**563 ± 74**	**622 ± 60**
	$\langle \mathbf{g(0,0)} \rangle$	0.86 ± 0.06	0.03 ± 0.01	0.22 ± 0.06	0.46 ± 0.13	0.37 ± 0.07

It is evident that in the presence of only the primary antibody of either Rab7 or LAMP-1, the intensities and the correlation amplitudes are very small compared to the samples where both are present, showing both that there is little background fluorescence and little, if any cross reactivity. In the presence of only the secondary antibody of either Rab7 or LAMP-1, the fluorescence intensities are slightly higher, indicating some non-specific binding, but still no significant cross reactivity. In these cases, the amplitude of the correlation function is not small, which allows estimates of the proportionality constant, c, and hence the absolute degrees of aggregation in some cases.

The same experiments were conducted on A549 cells with similar results.

Control for Cross-Talk between channels measured in C2C12 Cells

Cross-talk arises in the multiple-label experiments if irradiation in one channel is detected in another channel. To control for possible cross-talk, the detectors were carefully set to detect wavelengths within specific ranges: 489-560 nm for the 488 channel, 561-620 nm for the 561 channel, and 633-697 nm for the 633 channel.

Figure S4 show representative images obtained from C2C12 cells labelled with primary and secondary antibodies against all three markers with distinct fluorophores - Rab5 (561), Rab7 (633), and LAMP-1 (488).

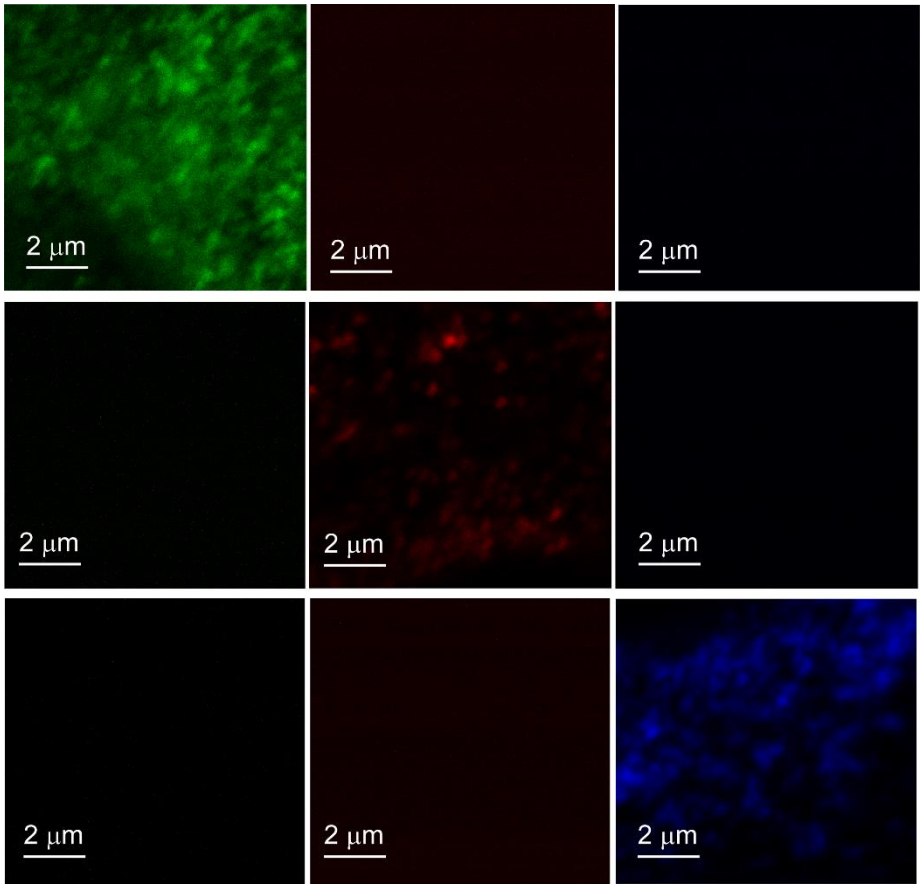

Figure S4: Representative Images in Cross-talk Experiments

Images A, D, and G were imaged in channel 488 (489-560 nm)
Images B, E, and H were imaged in channel 561 (561-620 nm)
Images C, F, and I were imaged in channel 633 (633-697 nm)
Images A, B, and C were excited with a 488 nm laser.
Images D, E, and F were excited with a 561 nm laser.
Images G, H, and I were excited with a 633 nm laser.

Significant fluorescence is observed only in those images where the excitation and observation wavelengths correspond, demonstrating that cross-talk is not a serious issue in these experiments.

Table S3 show the average values of intensities and correlation function amplitudes from ICS analysis of a few images corresponding to those shown in Figure S3, confirming that there is little significant cross-talk in under these experimental conditions.

Table S3: Average Intensities and Correlation Function Amplitudes for the Cross-talk Experiments.

	A	**B**	**C**
$\langle \boldsymbol{I}_{avg.} \rangle$	**940 ± 130**	13.7 ± 0.3	10.4 ± 0.1
$\langle \mathbf{g}(\mathbf{0},\mathbf{0}) \rangle$	0.10 ± 0.02	0.001 ± 0.000	0.002 ± 0.000
	D	**E**	**F**
$\langle \boldsymbol{I}_{avg.} \rangle$	9 ± 4	**191 ± 104**	8 ± 4
$\langle \mathbf{g}(\mathbf{0},\mathbf{0}) \rangle$	0.001 ± 0.000	0.3 ± 0.2	0.001 ± 0.00
	G	**H**	**I**
$\langle \boldsymbol{I}_{avg.} \rangle$	12.5 ± 0.1	12.6 ± 0.2	**439 ± 41**
$\langle \mathbf{g}(\mathbf{0},\mathbf{0}) \rangle$	0.01 ± 0.01	0.01 ± 0.01	0.4 ± 0.1

The same experiments were conducted on A459 cells with similar results.

References:

1. Keating, E., Brown, C. M. & Petersen, N. O. 16 - Mapping Molecular Interactions and Transport in Cell Membranes by Image Correlation Spectroscopy. in *Molecular Imaging* (eds. Periasamy, A. & Day, R. N.) 284–301 (American Physiological Society, 2005). doi:10.1016/B978-019517720-6.50025-0

2. St-Pierre, P. R. & Petersen, N. O. Average density and size of microclusters of epidermal growth factor receptors on A431 cells. *Biochemistry* **31**, 2459–2463 (1992).